Subharmonic resonances of the parametrically driven pendulum

Eugene I. Butikov
St. Petersburg State University, St. Petersburg, Russia

E-mail: butikov@spb.runnet.ru

Abstract. A simple qualitative physical explanation is suggested for the phenomenon of subharmonic resonances of a rigid planar pendulum whose axis is forced to oscillate with a high frequency in the vertical direction. An approximate quantitative theory based on the suggested approach is developed. The spectral composition of the subharmonic resonances is investigated quantitatively, and the boundaries of these modes in the parameter space are determined. New related modes of regular behaviour are described and explained. The conditions of the inverted pendulum stability are determined with a greater precision than they have been known earlier. A computer program simulating the physical system supports the analytical investigation.

PACS numbers: 5.45.-a, 05.10.-a, 07.05.Tp, 45.10.-b

1. Introduction: The physical system

An ordinary rigid planar pendulum whose axis is driven periodically in the vertical direction is a paradigm of contemporary nonlinear dynamics. This rather simple mechanical system is also interesting because the differential equation of the pendulum is frequently encountered in various problems of modern physics. Mechanical analogues of physical systems allow a direct visualization of motion and thus can be very useful in gaining an intuitive understanding of complex phenomena [1]. Depending on the frequency and amplitude of forced oscillations of the suspension point, this seemingly simple mechanical system exhibits a rich variety of nonlinear phenomena characterized by amazingly different types of motion.

When the external driving frequency is approximately twice the natural frequency of the pendulum, the lower state of equilibrium becomes unstable, and the system leaves it executing oscillations whose amplitude increases progressively. This commonly known phenomenon is called parametric resonance. In contrast to the case of ordinary resonance caused by a direct influence of some periodic external force, friction is unable to restrict the growth of parametrically excited oscillations. The growth of the amplitude is restricted because the period of natural oscillations increases with the amplitude due to nonlinear properties of the pendulum.

Besides the principal parametric resonance, excited when two driving cycles occur approximately during one natural oscillation, parametric resonances of higher orders are possible when two driving cycles occur approximately during two, three and any other integer number of natural periods. At small (and moderate) driving

amplitudes, parametrically excited oscillations in all these cases are very much like the natural ones – their frequency is close to the natural frequency of the pendulum. The forced oscillation of the pivot at resonant conditions supplies the pendulum with energy needed to compensate for frictional losses, thus preventing these almost natural oscillations from damping. With increasing friction, parametric resonances of higher orders become weaker and disappear.

Another possible kind of regular behaviour of the pendulum is a synchronized non-uniform unidirectional rotation in a full circle with a period that equals either the driving period or an integer multiple of this period. More complicated regular modes of the parametrically forced pendulum are formed by combined rotational and oscillatory motions synchronized (locked in phase) with oscillations of the pivot. Different competing modes can coexist at the same values of the driving amplitude and frequency. Which of these modes is eventually established when the transient is over depends on the starting conditions.

Behaviour of the pendulum whose axis is forced to oscillate with a frequency from certain intervals (and at large enough driving amplitudes) can be irregular, chaotic. Chaotic behaviour of this simple nonlinear system has been a subject of intense interest during recent decades [2] – [7]. The parametrically forced pendulum can serve as an excellent physical model for studying chaos as well as various complicated modes of regular behaviour.

An interesting feature in the behaviour of a rigid pendulum whose suspension point is forced to vibrate with a high frequency along the vertical line is the dynamic stabilization of its inverted position. When the frequency and amplitude of these vibrations are large enough, the inverted pendulum shows no tendency to turn down. Moreover, at small and moderate deviations from the vertical inverted position the pendulum tends to return to it. Being deviated, it can execute relatively slow oscillations about the vertical line on the background of rapid oscillations of the suspension point. This now well-known curiosity of classical mechanics, probably first pointed out by Stephenson [8] in 1908, has been explained physically and investigated experimentally in detail by Pjotr Kapitza [9] in 1951. Not surprisingly, since then this intriguing system has attracted attention of many researchers, and the theory of the phenomenon may seem to be well elaborated – see, for example, Landau [10]. Nevertheless, more and more new features in the behaviour of this apparently inexhaustible system are reported regularly. Further discoveries concerning general features and details in the behaviour of parametrically excited inverted pendulum have been published over the last decade [11] – [18].

Among these recent discoveries, the most important are the destabilization of the (dynamically stabilized) inverted position at large driving amplitudes through excitation of period-2 ("flutter") oscillations (Blackburn, 1992) [11], and the existence of n-periodic "multiple-nodding" regular oscillations (Acheson, 1995) [13]. However, the authors who discovered these interesting modes have not suggested any clear physical explanation to the origin of such "flutter" oscillations, as well as to the "multiple-nodding" oscillations. In this paper we present a quite simple qualitative physical explanation to these phenomena, and indicate the regions in the parameter space where these modes can exist. We show that the period-2 mode (the "flutter" oscillation) is closely (intimately) related to the commonly known parametric instability of the non-inverted pendulum, and that the "multiple-nodding" oscillations (which exist both for the inverted and hanging down pendulums) can be treated as high order subharmonic resonances of the parametrically driven pendulum. We

focus also on an approximate quantitative theory (leading to the well-known concept of the effective potential for the slow motion of the pendulum) which can be developed on the basis of the suggested approach to the problem. The coexistence of subharmonic resonances of different orders is explained. The spectral composition of these modes is investigated quantitatively. Conditions of the dynamical stability of the inverted pendulum are established with a greater precision than they have been known earlier. A computer program simulating the physical system supports the analytical investigation. The simulation reveals subtle details of the motion and aids the analytical study of the subject in a manner that is mutually reinforcing. The simulation program runs on a PC under MS Windows operating system and is available through the Web [19].

The paper is organized as follows. After introducing the physical system we consider briefly the pendulum's behaviour in the case of rapid oscillations of the pivot including dynamical stabilization of the inverted pendulum, which is important for understanding the origin of subharmonic resonances ("multiple-nodding" oscillations). Then we investigate the spectral composition of subharmonic resonances in the low-amplitude limit and determine the boundaries of the region in the parameter space in which these resonances can exist. Next we consider the destabilization of the dynamically stabilized pendulum (the "flutter" mode) and its relationship with ordinary parametric resonance. Then the influence of friction is taken into account. We report also for the first time about several new types of regular behaviour of the parametrically driven pendulum discovered with the help of computer simulations.

2. The physical model

For simplicity we consider a light rigid rod of length l with a heavy small bob of mass m on its end and assume that the rod has zero mass. Let the axis of the pendulum be forced to execute a given harmonic oscillation along the vertical line with a frequency ω and an amplitude a, i.e., let the motion of the axis be described by the following equation:

$$z(t) = a \sin \omega t \quad \text{or} \quad z(t) = a \cos \omega t. \tag{1}$$

Depending on the problem under consideration, either sine or cosine time dependence may be more convenient for calculations. The force of inertia $F_{\text{in}}(t) = -m\ddot{z}(t) = m\omega^2 z(t)$ exerted on the bob in the non-inertial frame of reference associated with the pivot also has the same sinusoidal dependence on time. This force is equivalent to a periodic modulation of the force of gravity exerted on the pendulum. If the frequency and/or amplitude of the pivot are large enough (if $a\omega^2 > g$), for some part of the driving period the apparent gravity is even directed upward.

An understanding about pendulum's behaviour in the case of rapid oscillations of its pivot is an important prerequisite for the physical explanation of subharmonic resonances ("multiple-nodding" oscillations). Details of the physical mechanism responsible for the dynamical stabilization of the inverted pendulum can be found in [20]. The principal idea is utterly simple: Although the mean value of the force of inertia $F_{\text{in}}(t)$, averaged over the short period of these oscillations, is zero, the averaged over the period value of its *torque* about the axis is not zero. The reason is that both the force $F_{\text{in}}(t)$ and the *arm* of this force vary with time in the same way synchronously with the axis' vibrations. This non-zero mean torque tends to align the pendulum along the direction of forced oscillations of the axis. For given values of the

driving frequency and amplitude, the mean torque of the force of inertia depends only on the angle of the pendulum's deflection from the direction of the pivot's vibration.

In the absence of gravity the inertial torque gives a clear physical explanation for existence of the two equivalent stable equilibrium positions that correspond to the two preferable orientations of the pendulum's rod along the direction of the pivot's vibration. With gravity, the inverted pendulum is stable with respect to small deviations from this position provided the mean torque of the force of inertia is greater than the torque of the force of gravity that tends to tip the pendulum down. This occurs when the following condition is fulfilled: $a^2\omega^2 > 2gl$, or $(a/l)(\omega/\omega_0) > \sqrt{2}$ (see, e.g., [20]). However, this is only an approximate criterion for dynamic stability of the inverted pendulum, which is valid at small amplitudes of forced vibrations of the pivot ($a \ll l$). Below we establish a more precise criterion [see equation (12)].

To provide the dynamic stabilization of the inverted pendulum within some finite interval of the angles of deflection from the vertical position, the product of the normalized driving amplitude and the normalized driving frequency must be greater than $\sqrt{2}$ by a finite value. We note that the explanation of the physical reason for the dynamic stabilization of the inverted pendulum in [20] is free from the restriction of small angles. In particular, for given values of the driving frequency ω and amplitude a, this approach allows us to find the maximal admissible angular deflection from the inverted vertical position $\theta_{\max}$ below which the pendulum tends to return to this position, even when $\theta_{\max}$ is almost as large as $\pi/2$: $\cos\theta_{\max} = 2gl/(a^2\omega^2)$. Being deflected from the vertical position by an angle that does not exceed $\theta_{\max}$, the pendulum will execute relatively slow oscillations about this inverted position. This motion is executed both under the mean torque of the force of inertia and the force of gravity, and can be described by a slow-varying function $\psi(t)$ satisfying the following approximate differential equation (if friction is ignored):

$$\ddot{\psi} + \omega_0^2 \sin\psi + \frac{1}{2}\frac{a^2}{l^2}\omega^2 \cos\psi \sin\psi = 0. \tag{2}$$

Rapid oscillations caused by forced vibrations of the axis superimpose on this slow motion of the pendulum. With friction, the slow motion gradually damps, and the pendulum wobbles up settling eventually in the inverted position.

Similar behaviour of the pendulum can be observed when it is deflected from the lower vertical position. But in this case the frequency of the smooth slow oscillations is greater than for the inverted pendulum. The frequencies ω_{up} and ω_{down} of small slow oscillations about the inverted position and the lower vertical position are given by the following expressions:

$$\omega_{\text{up}}^2 = \omega^2(a/l)^2/2 - \omega_0^2, \qquad \omega_{\text{down}}^2 = \omega^2(a/l)^2/2 + \omega_0^2. \tag{3}$$

Substituting $\omega_0 = 0$ into these formulas, we get the expression $\omega_{\text{slow}} = \omega(a/l)/\sqrt{2}$ for the frequency of small slow oscillations of the pendulum with vibrating axis in the absence of the gravitational force. These oscillations can occur about any of the two equivalent dynamically stabilized equilibrium positions located opposite one another along the direction of forced vibrations of the axis.

Experimental verification of equations (3) is given by the graphs in Figure 1, obtained in the simulation. In this example the driving frequency $\omega = 16\omega_0$ and the driving amplitude $a = 0.153\,l$, so that $(a^2/2l^2)\omega^2 = 3\omega_0^2$. Thus equation (3) provides for the frequency of slow oscillations about the downward position the value

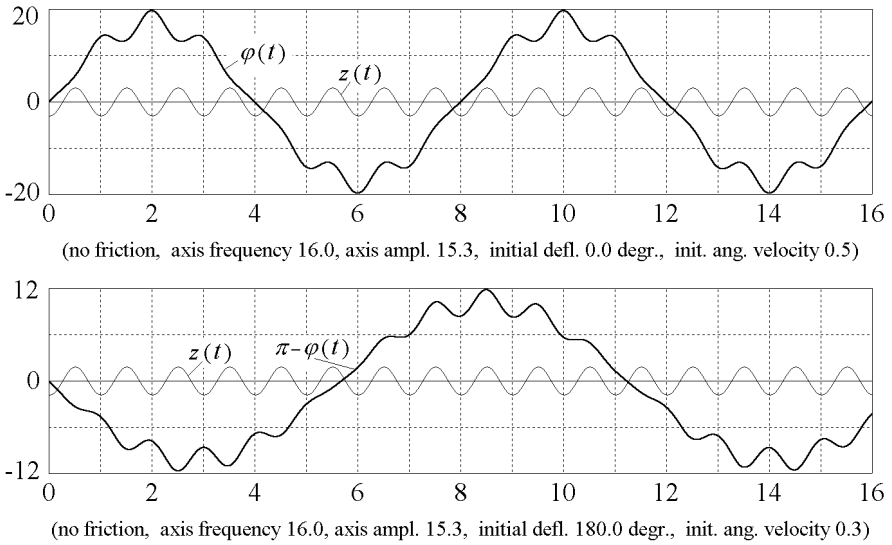

Figure 1. The graphs of oscillations of the rigid planar pendulum with vibrating axis about the dynamically stabilized lower and upper equilibrium positions respectively, obtained by a numerical integration of the exact differential equation, equation (5), for the momentary angular deflection $\varphi(t)$. The sinusoidal graphs of the axis motion $z(t) = -a\cos\omega t$ are shown by thin lines.

$\omega_{\rm down} = 2\omega_0$ that is exactly twice the natural frequency ($T_{\rm down} = T_0/2$), while for the frequency of slow oscillations about the upward vertical position $\omega_{\rm up} = \sqrt{2}\omega_0$ ($T_{\rm up} = T_0/\sqrt{2}$). The graphs in Figure 1 agree well with these values (two periods $T_{\rm down}$ of slow oscillation about hanging position are completed during exactly one natural period T_0 that equals $16T$).

The graphs in Figure 1 also show clearly that the smooth motion is distorted by the high frequency oscillations most of all near the utmost deflections of the pendulum, and these distortions are relatively small while the pendulum crosses the equilibrium position. This implies that the momentary deflection angle $\varphi(t)$ can be represented approximately as a superposition of the slow varying mean angle $\psi(t)$ and the high frequency term whose angular amplitude is proportional to sine of $\psi(t)$:

$$\varphi(t) \approx \psi(t) - (z/l)\sin\psi(t) = \psi(t) - (a/l)\sin\psi(t)\sin\omega t. \tag{4}$$

Indeed, the angular amplitude of the rapid (second) term in equation (4) is the greatest at the extreme deflections of the pendulum, and this amplitude vanishes when the pendulum in its smooth motion crosses each of the vertical positions. An observer that doesn't notice the rapid oscillating motion of the pendulum can consider simply that the system moves in an effective potential field $U = U(\psi)$. Such a potential function that governs the smooth motion of the pendulum averaged over the rapid oscillations was first introduced by Landau [10], and derived by several different methods afterwards (see, for example, [14], [15], or [20]). Certainly, some subtle details in the motion of the pendulum revealed by the simulations are lost in the approximate analysis, which refers only to the slow component of the investigated motion. Nevertheless, this analysis allows us to clearly interpret the

principal features of the physical system under consideration, and even to evaluate such typically nonlinear properties as the dependence of the period on the amplitude of slow oscillations.

The simulation is based on a numerical integration of the exact differential equation for the momentary angular deflection $\varphi(t)$. This equation includes, beside the torque of the force of gravity, the instantaneous (not averaged over the fast period) value of the torque exerted on the pendulum by the force of inertia that depends explicitly on time t:

$$\ddot{\varphi} + 2\gamma\dot{\varphi} + (\omega_0^2 - \frac{a}{l}\omega^2 \sin\omega t)\sin\varphi = 0. \tag{5}$$

The second term of equation (5) takes into account the braking frictional torque, assumed to be proportional to the momentary angular velocity $\dot{\varphi}$ in the mathematical model of the simulated system. The damping constant γ is inversely proportional to the quality factor Q commonly used to characterize the viscous friction: $Q = \omega_0/2\gamma$. In the absence of gravity the parametrically driven pendulum is described by equation (5) with $\omega_0 = 0$. Since in this case the notion of natural frequency loses its sense, it is impossible to use the quality factor defined as $Q = \omega_0/2\gamma$ to characterize friction, but instead we can use another dimensionless quantity $\omega/2\gamma$, where ω is the driving frequency.

We note that oscillations about the inverted position can be formally described by the same differential equation, equation (5), with negative values of $\omega_0^2 = g/l$. In other words, we can consider ω_0^2 as a control parameter whose variation is physically equivalent to changing the gravitational force exerted on the pendulum. When this control parameter is diminished through zero to negative values, the constant (gravitational) torque in equation (5) first turns to zero and then changes its sign to the opposite. Such a "gravity" tends to bring the pendulum into the inverted position $\varphi = \pi$, destabilizing the position $\varphi = 0$ of the unforced pendulum: The inverted position with $\omega_0^2 < 0$ in equation (5) is equivalent to the hanging down position with the positive value of ω_0^2 of the same magnitude.

3. Subharmonic resonances of high orders

When the driving amplitude and frequency lie within certain ranges, the pendulum, instead of gradually approaching the equilibrium position (either dynamically stabilized inverted position or ordinary downward position) by the process of damped slow oscillations, can be trapped in a n-periodic limit cycle locked in phase to the rapid forced vibration of the axis. In such oscillations the phase trajectory repeats itself after n driving periods T. Since the motion has period nT, and the frequency of its fundamental harmonic equals ω/n (where ω is the driving frequency), this phenomenon can be called a subharmonic resonance of n-th order. For the inverted pendulum with a vibrating pivot, periodic oscillations of this type were first described by Acheson [13], who called them "multiple-nodding" oscillations. An example of such stationary oscillations whose period equals ten periods of the axis is shown in Figure 2.

The left-hand upper part of the figure shows the spatial trajectory of the pendulum's bob at these multiple-nodding oscillations. The left-hand lower part shows the closed looping trajectory in the phase plane (φ, $\dot{\varphi}$). In the absence of friction the backward motion of the pendulum occurs along the same path, and the phase trajectory has the symmetry of reflection about the axes. Right-hand side of Figure 2,

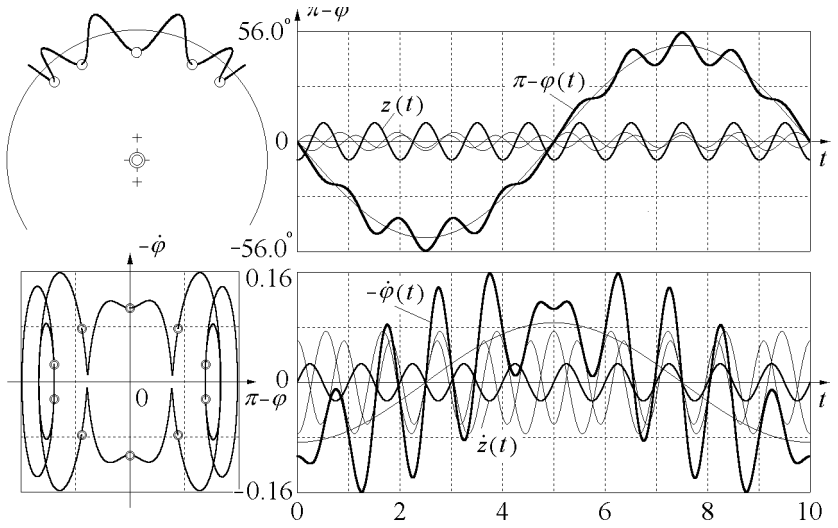

Figure 2. The spatial path, phase orbit with Poincaré sections, and graphs of stationary period-10 oscillations. The graphs are obtained by a numerical integration of the exact differential equation, equation (5) with $\omega_0 = 0$ and $\gamma = 0$, for the momentary angular deflection $\varphi(t)$. Thin lines show separate harmonics. The fundamental harmonic with the frequency $\omega/10$ dominates in the spectrum. The 9th and 11th harmonics have nearly equal amplitudes. Graphs of the axis motion $z(t)$ and $\dot{z}(t)$ are also shown.

alongside the graphs of $\varphi(t)$ and $\dot{\varphi}(t)$, shows also their harmonic components and the graphs of the pivot oscillations. The fundamental harmonic whose period equals ten driving periods dominates in the spectrum. We may treat it as a subharmonic (as an "undertone") of the driving oscillation. This harmonic describes the discussed above smooth component of the compound period-10 oscillation.

Next we show that the approximate approach based on the effective potential for the slow motion provides a simple qualitative physical explanation for such an extraordinary and even counterintuitive at first sight behaviour of the pendulum. Moreover, for subharmonic resonances with $n \gg 1$ this approach yields rather good quantitative results.

First of all we emphasize that these modes of regular n-periodic oscillations (subharmonic resonances), which have been discovered (see [13]) in investigations of the dynamically stabilized inverted pendulum with a vibrating pivot, are not specific for the inverted pendulum. Similar oscillations can be executed also (at appropriate values of the driving parameters) about the ordinary (downward hanging) equilibrium position. Actually, the origin of subharmonic resonances is independent of gravity, because such synchronized with the pivot "multiple-nodding" oscillations can occur also in the absence of gravity about any of the two equivalent dynamically stabilized equilibrium positions of the pendulum with a vibrating axis. Even the pendulum with the horizontally vibrating pivot can execute similar n-periodic oscillations about each of the two lateral equilibrium positions that are displaced downward by the

gravitational force from the horizontal line of the pivot's oscillations.‡

The natural slow oscillatory motion in the effective potential well is almost periodic (exactly periodic in the absence of friction). A subharmonic resonance of order n can occur if one cycle of this slow motion covers approximately n driving periods, that is, when the driving frequency ω is close to an integer multiple n of the natural frequency of slow oscillations near either the inverted or the ordinary equilibrium position: $\omega = n\omega_{\rm up}$ or $\omega = n\omega_{\rm down}$. In this case the phase locking can occur, in which one cycle of the slow motion is completed *exactly* during n driving periods. Synchronization of these modes with the oscillations of the pivot creates conditions for systematic supplying the pendulum with the energy needed to compensate for dissipation, and the whole process becomes exactly periodic.

For small amplitudes of the slow oscillations, each of the minima of the effective potential can be approximated by a parabolic well in which the smooth component of motion is almost harmonic. Equating $\omega_{\rm slow}$ to ω/n, we find the threshold (low-amplitude) conditions for the subharmonic resonance of order n. As an example how the approach based on the effective potential allows us to explain properties of these n-periodic oscillations and predict conditions at which they can occur, we consider first the simplest case of the pendulum in the absence of gravity, or, which is essentially the same, the limiting case of very high driving frequencies $\omega \gg \omega_0$ ($\omega/\omega_0 \to \infty$). In this limit both equilibrium positions (ordinary and inverted) are equivalent, and the normalized driving amplitude $m = a/l$ is the only parameter to be predicted as a required condition of the subharmonic resonance of order n (of synchronized with the pivot n-periodic oscillations of the pendulum). According to equation (3), at $\omega_0 = 0$ the frequency of slow oscillations is given by $\omega_{\rm slow}/\omega = m/\sqrt{2}$, whence for the subharmonic resonance of order n, at which the period of the slow motion equals n periods of the axis, $m_{\rm min} = \sqrt{2}/(\omega/\omega_{\rm slow}) = \sqrt{2}/n$. For the subharmonic resonance of 10th order ($n = 10$) shown in Figure 2 we find $m_{\rm min} = \sqrt{2}/10 = 0.141$. This value is rather close to the predictions of a more precise theory of the boundaries for these modes based on the linearized differential equation of the system (see equation (13) below), which gives for such period-10 small oscillations in the absence of gravity the normalized driving amplitude $m_{\rm min} = 99/(50\sqrt{202}) = 0.139$. The latter value agrees perfectly well with the simulation experiment in conditions of small amplitudes.

In the presence of gravity, assuming $\omega_{\rm down,\,up} = \omega/n$ (n driving cycles during one cycle of the slow oscillation), we find for the minimal normalized driving amplitudes (for the boundaries of the subharmonic resonances) the values

$$m_{\rm min} = \sqrt{2(1/n^2 \mp k)}, \tag{6}$$

where $k = (\omega_0/\omega)^2$. As we already indicated above, negative values of the parameter k (negative ω_0^2 values) can be treated as referring to the inverted pendulum. Then the boundaries of subharmonic resonances can be expressed both for the hanging down and inverted pendulum by the same formula: $m_{\rm min} = \sqrt{2(1/n^2 - k)}$. The limit of this expression at $n \to \infty$ gives the mentioned earlier approximate condition of stability of the inverted pendulum: $m_{\rm min} = \sqrt{-2k}$ (where $k < 0$).

Being based on a decomposition of motion on slow oscillations and rapid vibrations with the driving frequency, equation (6) is approximate and valid if the

‡ At horizontal forcing of the pivot the hanging down vertical equilibrium position destabilizes and two symmetric lateral dynamically stabilized equilibrium positions appear if the driving amplitude and frequency satisfy the same condition that corresponds to the dynamic stabilization of the inverted pendulum at vertical forcing.

amplitude of constrained vibration of the axis is small compared to the pendulum's length ($a \ll l$). Moreover, in the presence of gravity the driving frequency must be much greater than the frequency of small natural oscillations of the pendulum ($\omega \gg \omega_0$). These restrictions mean that we should not expect from the discussed here approach to give an exhaustive description of the parametrically driven pendulum in all cases.

In particular, within certain ranges of the system parameters (in the intervals of parametric instability) the lower position of the pendulum becomes unstable, as we already mentioned earlier. However, parametric resonance, as well as the modes of chaotic behaviour, occur at such driving frequencies (for the principal parametric resonance $\omega \approx 2\omega_0$) that do not satisfy the conditions of applicability of the approach used above. Next we show how to get instead of equation (6) the exact condition for the boundaries of the subharmonic resonances.

The spectrum of stationary n-period oscillations consists primarily of the fundamental harmonic $A\sin(\omega t/n)$ with the frequency ω/n, and two high harmonics of the orders $n-1$ and $n+1$. Indeed, according to equation (4) with $\sin\psi \approx \psi$, in this approximation

$$\begin{aligned}\varphi(t) &= \psi(t) - m\sin\psi\cos\omega t \approx \psi(t) - m\psi\cos\omega t = \\ &= A\sin(\omega t/n) - mA\sin(\omega t/n)\cos\omega t = \\ &= A\sin(\omega t/n) - (mA/2)\sin[(n-1)\omega t/n] + (mA/2)\sin[(n+1)\omega t/n].\end{aligned} \tag{7}$$

This spectral composition is clearly seen from the plots in Figure 2. While the pendulum crosses the equilibrium position, both high harmonics add in the opposite phases and thus almost don't distort the smooth motion (described by the principal harmonic). Near the utmost deflections the phases of high harmonics coincide, and thus here their sum causes the most serious distortions of the smooth motion.

According to equation (7), both high harmonics have equal amplitudes $(m/2)A$. However, we see from the plots in Fig. 2 that these amplitudes are slightly different. Therefore we can try to improve the approximate solution for $\varphi(t)$, equation (7), as well as the theoretical values for the lower boundaries of subharmonic resonances, equation (6), by assuming for the possible solution a similar spectrum but with unequal amplitudes, A_{n-1} and A_{n+1}, of the two high harmonics (for $n > 2$, the case of $n = 2$ will be considered separately):

$$\varphi(t) = A_1\sin(\omega t/n) + A_{n-1}\sin[(n-1)\omega t/n] + A_{n+1}\sin[(n+1)\omega t/n]. \tag{8}$$

Since oscillations at the boundaries have infinitely small amplitudes, we can use instead of equation (5) the following linearized (Mathieu) equation:

$$\ddot{\varphi} + 2\gamma\dot{\varphi} + (\omega_0^2 - m\omega^2\sin\omega t)\varphi = 0. \tag{9}$$

Substituting $\varphi(t)$, equation (8), into this equation (with $\gamma = 0$) and expanding the products of trigonometric functions, we obtain a system of approximate equations for the coefficients A_1, A_{n-1} and A_{n+1}:

$$\begin{aligned} 2(kn^2-1)A_1 + mn^2A_{n-1} - mn^2A_{n+1} &= 0, \\ mn^2A_1 + 2[n^2(k-1)+2n-1]A_{n-1} \quad &= 0, \\ -mn^2A_1 + 2[n^2(k-1)-2n-1]A_{n+1} &= 0. \end{aligned} \tag{10}$$

The homogeneous system has a nontrivial solution if its determinant equals zero. This condition yields an equation for the corresponding critical (minimal) driving

amplitude $m_{\min}$ at which n-period mode $\varphi(t)$, equation (8), can exist. Solving the equation, we find:

$$m_{\min}^2 = \frac{2}{n^4}\frac{[n^6k(k-1)^2 - n^4(3k^2+1) + n^2(3k+2) - 1]}{[n^2(1-k)+1]}. \qquad (11)$$

Then, for this critical driving amplitude $m_{\min}$, the fractional amplitudes A_{n-1}/A_1 and A_{n+1}/A_1 of high harmonics for a given order n can be easily found as the solutions to the homogeneous system of equations, equations (10).

The limit of $m_{\min}$, equation (11), at $n \to \infty$ gives an improved formula for the lower boundary of the dynamic stabilization of the inverted pendulum instead of the commonly known (and mentioned above) approximate criterion $m_{\min} = \sqrt{-2k}$:

$$m_{\min} = \sqrt{-2k(1-k)} \qquad (k < 0). \qquad (12)$$

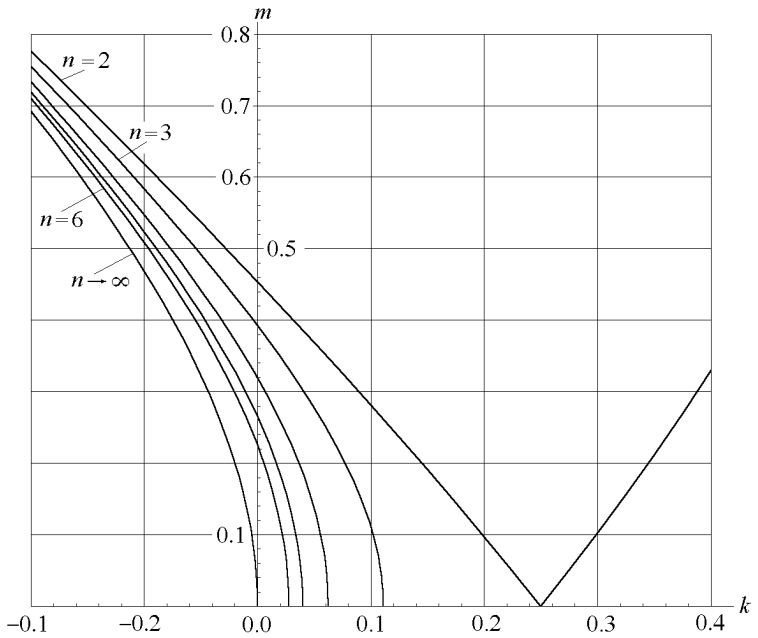

Figure 3. The normalized driving amplitude $m = a/l$ versus $k = (\omega_0/\omega)^2$ (inverse normalized driving frequency squared) at the boundaries of the dynamic stabilization of the inverted pendulum (the left curve marked as $n \to \infty$), and at subharmonic resonances of several orders n (see text for detail).

The minimal amplitude $m_{\min}$ that provides the dynamic stabilization is shown as a function of $k = (\omega_0/\omega)^2$ (inverse normalized driving frequency squared) by the left curve ($n \to \infty$) in Figure 3. The other curves to the right from this boundary show the dependence on k of minimal driving amplitudes for which the subharmonic resonances of several orders can exist (the first curve for $n = 6$ and the others for n values diminishing down to $n = 2$ from left to right). At positive values of k these curves correspond to the subharmonic resonances of the hanging down parametrically excited pendulum. Subharmonic oscillations of a given order n (for $n > 2$) are possible to the left of $k = 1/n^2$, that is, for the driving frequency $\omega > n\omega_0$. The curves in

Figure 3 show that as the driving frequency ω is increased beyond the value $n\omega_0$ (i.e., as k is decreased from the critical value $1/n^2$ toward zero), the threshold driving amplitude (over which n-order subharmonic oscillations are possible) rapidly increases. The limit of very high driving frequency ($\omega/\omega_0 \to \infty$), in which the gravitational force is insignificant compared with the force of inertia (or, which is essentially the same, the limit of zero gravity $\omega_0/\omega \to 0$), corresponds to $k = 0$, that is, to the points of intersection of the curves in Figure 3 with the m-axis. The continuations of these curves further to negative k values describe the transition through zero gravity to the "gravity" directed upward, which is equivalent to the case of an inverted pendulum in ordinary (directed downward) gravitational field. Therefore these curves at negative k values give the threshold driving amplitudes for subharmonic resonances of the inverted pendulum.§

A complete investigation of the parametrically excited pendulum is complicated by the extensive set of parameters that characterize the system (ω_0, ω, a, γ). A considerable simplification is achieved by eliminating one the parameters, namely, the natural frequency $\omega_0 = \sqrt{g/l}$, when we turn to studying the pendulum in the absence of gravity. This simplified model is also useful for qualitative understanding of the pendulum's behaviour in the presence of gravity in cases of high driving frequency and/or large driving amplitude, when the gravitational force plays the role of a small addition to the force of inertia. Many of the mentioned above complicated counterintuitive modes are not related to the force of gravity, and can be studied in their purest form when they are observed in the simple device with the oscillating pivot in the absence of gravity, which is described by equation (5) with $\omega_0 = 0$.

The points of intersection of the curves in Figure 3 with the m-axis, corresponding to the threshold conditions at zero gravity ($k = 0$), give, according to equation (11), the following values of the normalized driving amplitudes:

$$m_{\min} = \frac{\sqrt{2}(n^2-1)}{n^2\sqrt{n^2+1}}. \tag{13}$$

The fractional amplitudes A_{n-1}/A_1 and A_{n+1}/A_1 of the most important high harmonics of $\varphi(t)$ [expressed approximately by equation (8)] for the case of zero gravity ($k = 0$) are given by the following formulas:

$$\frac{A_{n-1}}{A_1} = \frac{n+1}{\sqrt{2}\sqrt{n^2+1}(n-1)}, \quad \frac{A_{n+1}}{A_1} = \frac{n-1}{\sqrt{2}\sqrt{n^2+1}(n+1)}. \tag{14}$$

These theoretical values for the boundaries $m_{\min}$ and amplitudes of high harmonics A_{n-1}/A_1 and A_{n+1}/A_1 for resonances of different orders n agree well with the simulation experiments. Over the boundaries additional components appear in the spectrum of resonant oscillations (see below). Figures 4 – 5 show the graphs of subharmonic oscillations for $n = 8$ and $n = 6$; Figures 8 – 10 show the graphs for $n =$ 5, 4, and 3, obtained in the simulations.

For subharmonic resonances of high orders ($n \gg 1$), equation (13) in the case of zero gravity yields the approximate value $m_{\min} \approx \sqrt{2}/n$ obtained earlier with the help of the simple approach which treats the condition of n-order subharmonic resonance as the coincidence of n driving periods with one period of the slow motion of the pendulum near the bottom of the effective potential well. The fractional

§ Actually the curves in Figure 3 are plotted not according to equation (11), but rather with the help of a somewhat more comlicated formula (not cited in this paper), which is obtained by holding one more high order harmonic component in the trial function $\varphi(t)$.

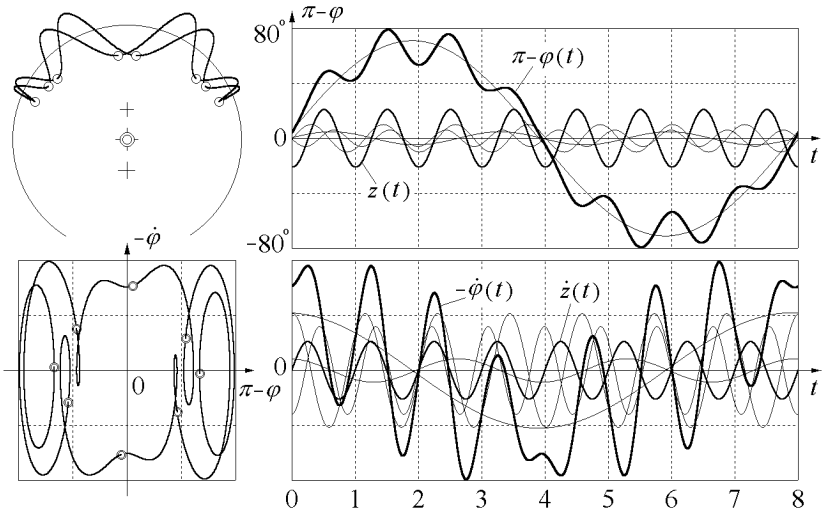

(quality 400.0, no gravity, axis amplitude 0.265, initial defl. 175.51 degr., init. ang. velocity -0.2284)

Figure 4. The spatial path, phase orbit with Poincaré sections, and graphs of large-amplitude stationary period-8 oscillations. The fundamental harmonic with the frequency $\omega/8$ dominates in the spectrum. This harmonic describes the smooth (slow) motion of the pendulum. The most important high harmonics have frequencies $7\omega/8$ and $9\omega/8$. At large swing the third harmonic (frequency $3\omega/8$) is noticeable. This spectral component reflects the non-harmonic character of slow oscillations in the non-parabolic effective potential well.

amplitudes of both high harmonics A_{n-1}/A_1 and A_{n+1}/A_1, given by equation (14), at $n \gg 1$ are almost equal and approach to the common value $1/(\sqrt{2}n) = m_{\min}/2$, in accordance with equation (7) that describes the n-period subharmonic oscillations as a superposition of the slow and rapid motions.

With gravity, these complex n-periodic "multiple-nodding" modes exist both for the inverted and non-inverted pendulum.

4. Coexistence of subharmonic resonances with different n

Estimating conditions for n-periodic oscillations with the help of equation (3), we assume the slow motion of the pendulum in the effective potential well to be simple harmonic, which is true only if this motion is limited to a small vicinity of the bottom of this well. Therefore we get the lower limit for the driving amplitude at which n-periodic oscillations of only infinitely small amplitude can occur. Smooth non-harmonic oscillations of a finite angular excursion that extends over the slanting slopes of the non-parabolic effective potential well are characterized by a greater period than the small-amplitude harmonic oscillations executed just over the parabolic bottom of this well. Therefore large-amplitude period-8 oscillations shown in Figure 4 (their swing equals 80°) occur at a considerably greater value of the driving amplitude ($a = 0.265\,l$) than the critical (threshold) value $a_{\min} = 0.173\,l$.

For the oscillations of a large swing shown in Figure 4, the contribution of the 3rd harmonic to the spectrum is also noticeable. In our approximate approach, the appearance of this spectral component is explained by deviations in the shape of the

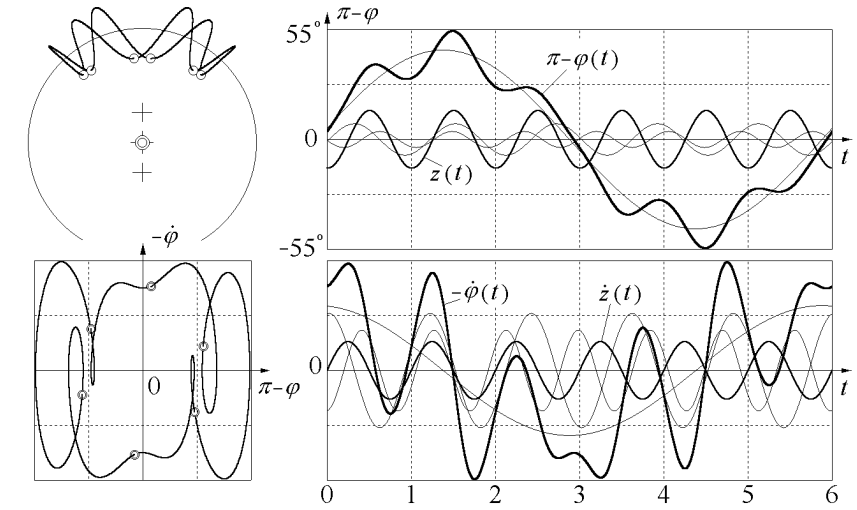

Figure 5. The spatial path, phase orbit, and graphs of period-6 stationary oscillations coexisting with period-8 oscillations (occurring at the same values of the pendulum and drive parameters as in figure 4).

effective potential well (in which the slow oscillation is executed) from a parabolic well, that is, by non-harmonic character of the slow oscillation with a large angular excursion. Moreover, because the smooth motion is executed in a non-parabolic effective potential well with a "soft" restoring force, the period becomes longer as the amplitude is increased. By virtue of this dependence of the period of non-harmonic smooth motion on the swing, several modes of subharmonic resonance with different values of n can coexist at the same amplitude and frequency of the pivot. Indeed, the period of a slow non-harmonic oscillation with some finite amplitude can be equal to, say, six driving periods, while the period of a slow oscillation with a somewhat greater amplitude in the same non-parabolic potential well can be equal to eight driving periods. Figures 4 and 5 show the simulations of such coexisting period-8 and period-6 modes respectively, obtained at identical parameters of the system. That is, both smooth motions occur in the same effective potential well. In which of these competing modes is the pendulum eventually trapped in a certain simulation, depends on the starting conditions. The set of initial conditions that leads, after an interval in which transients decay, to a given dynamic equilibrium (to the same steady-state periodic motion, or attractor) in the limit of large time, constitutes the basin of attraction of this attractor. The coexisting periodic motions in Figures 4 and 5 represent competing attractors and are characterized by different domains of attraction.

As noted earlier, in the case of period-8 oscillations of a small swing the approach based on the effective potential predicts (in the absence of gravity) for the driving amplitude $m = a/l$ a value of $\sqrt{2}/8 = 0.177$ which is rather close to the exact low-amplitude theoretical limit ($a/l = 0.173$). To obtain the slow oscillations of a smaller period (say, of six driving periods), we should increase the driving amplitude. Indeed, if $\omega_{\text{slow}} = \omega/6$, equation (3) yields a greater value $a/l = \sqrt{2}/6 = 0.236$. However,

for such period-6 oscillations this predicted threshold value agrees somewhat worse with the calculation based on the linearized equation of the system. According to equation (13), the minimal driving amplitude for period-6 small oscillations in the absence of gravity equals $a_{\min} = 35/(18\sqrt{74})\, l = 0.226\, l$. This value agrees perfectly with the simulation experiment. Not surprisingly, for the n-periodic oscillation with a small n we cannot expect good quantitative predictions from the effective potential approach because in such cases the period of a "smooth" motion contains only a few driving periods. The "rapid" component of the motion here is not rapid enough for good averaging.

Nevertheless, the effective potential approach provides us not only with a qualitative understanding of these complex periodic modes, but also, being applicable for large-amplitude motions, explains the coexistence of several n-periodic modes with different n values at identical system parameters. Figure 6 shows the dependence on the driving amplitude $m = a/l$ of the fundamental harmonic amplitudes A_1 for both $n = 8$ and $n = 6$ modes.

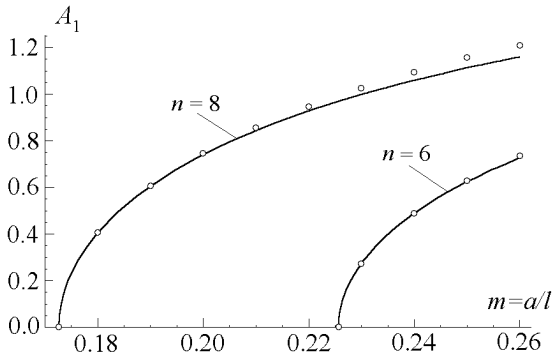

Figure 6. The principal harmonic amplitudes for $n = 8$ and $n = 6$ modes versus the driving amplitude $m = a/l$ given by an approximate theory (see text for detail) and by the simulation experiment.

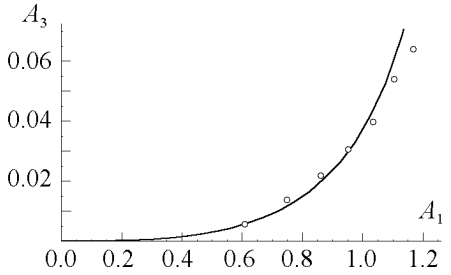

Figure 7. The third harmonic amplitude for $n = 8$ mode versus the amplitude of the principal harmonic given by the approximate theory (see text) and by the simulation experiment.

To estimate how the swing of oscillations executed at the subharmonic resonance of a given order n depends on the excess $a - a_{\min}$ of the driving amplitude a over the

critical (threshold) value $a_{\min}$, and how the fractional amplitude of the third harmonic depends on the swing, we can expand $\sin\psi$ and $\sin 2\psi$ in the differential equation that describes the slow motion, equation (2), in a power series, preserving the two first terms:

$$\ddot{\psi} + \omega_0^2(\psi - \frac{1}{6}\psi^3) + \frac{1}{2}m^2\omega^2(\psi - \frac{2}{3}\psi^3) = 0. \tag{15}$$

Here we use again the notation $m = a/l$ for the normalized driving amplitude. We can try to search for the solution of equation (15) in the form of a superposition of the fundamental and third harmonics:

$$\psi = A_1 \sin\omega_1 t + A_3 \sin 3\omega_1 t. \tag{16}$$

Substituting ψ, equation (16), into equation (15) and equating to zero the coefficient of $\sin\omega_1 t$, we find how the frequencies of slow oscillations depend on the amplitude A_1: $\omega^2_{\text{down, up}} = \frac{1}{2}m^2\omega^2(1 - \frac{1}{2}A_1^2) \pm \omega_0^2(1 - \frac{1}{8}A_1^2)$. This expression reduces to equation (3) if $A_1 \to 0$. Equating the frequencies $\omega_{\text{down, up}}$ to the fundamental harmonic frequency ω/n , we obtain an approximate dependence of the fundamental harmonic amplitude A_1 on the excess of the normalized driving amplitude over its critical value $m - m_{\min}$. For the case $\omega_0 = 0$ (absence of gravity) we find:

$$A_1 = \sqrt{2}\sqrt{1 - m^2_{\min}/m^2} \approx 2\sqrt{1 - m_{\min}/m}. \tag{17}$$

The latter approximate expression is valid if the driving amplitude only moderately exceeds the critical value (if $m - m_{\min} \ll m_{\min}$). For $n = 8$ and $n = 6$ the dependencies of A_1 on m are plotted by solid curves in Figure 6 together with experimental values of A_1 obtained by numerical simulations. If the driving amplitude m is greater than $m_{\min} = 0.226$ for $n = 6$, each of the subharmonic oscillations with $n = 8$ and $n = 6$ can exist at the same values of the driving parameters.

The amplitude A_3 of the third harmonic in equation (16) can be estimated similarly by equating to zero the coefficient of $\cos 3\omega_1 t$, when ψ from equation (16) is substituted into equation (15). It is convenient to express A_3 as a function of the amplitude A_1 of the slow motion: $A_3 = \frac{1}{3}A_1^3/(16 - 7A_1^2)$. The corresponding graph is shown by a solid line in Figure 7. The points refer to the simulation of the subharmonic oscillations with $n = 8$.

Friction introduces a phase shift between forced oscillations of the pivot and harmonics of the steady-state n-periodic motion of the pendulum. By virtue of this phase shift the pendulum is supplied with energy needed to compensate for frictional losses. With friction, the direct and backward spatial paths of the pendulum do not coincide, and the symmetry of the phase trajectory with respect to the ordinate axis is destroyed. This is clearly seen from a comparison of Figures 4 or 5 for subharmonic resonances in the presence of weak friction with Figure 2, which refers to an idealized case in which friction is absent.

5. The upper boundary of the dynamic stability and the principal parametric resonance

When the amplitude a of the pivot vibrations is increased beyond a certain critical value $a_{\max}$, the dynamically stabilized inverted position of the pendulum loses its stability. After a disturbance the pendulum does not come to rest in the up position, no matter how small the release angle, but instead eventually settles into a finite

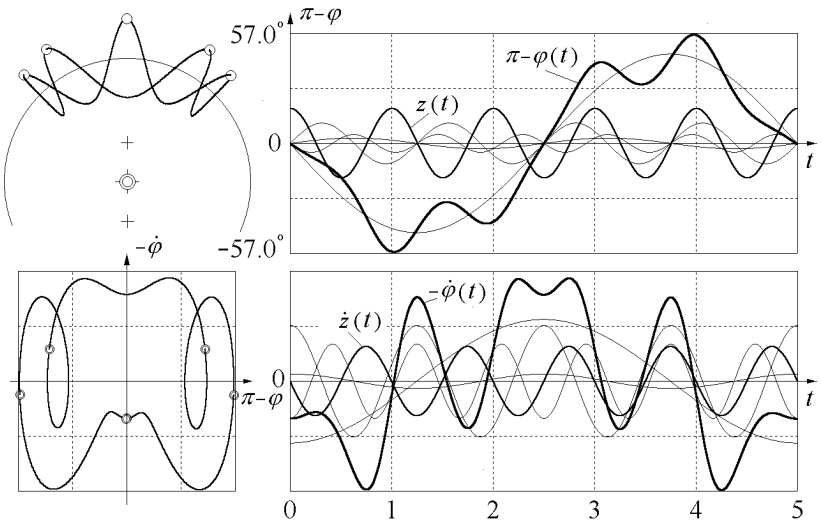

(no friction, no gravity, axis amplitude 0.319, initial defl. 180.0 degr., init. ang. velocity 0.1)

Figure 8. The spatial path, phase orbit with Poincaré sections, and graphs of period-5 oscillations. The graphs are obtained by a numerical integration of the exact differential equation, equation (5), for the momentary angular deflection of the pendulum $\varphi(t)$. Separate harmonics are shown by thin lines. The fundamental harmonic (frequency $\omega/5$) dominates in the spectrum. Next the 4th and 6th harmonics (frequencies $4\omega/5$ and $6\omega/5$) contribute to a considerable extent. At large swing the second harmonic (frequency $2\omega/5$) is also noticeable.

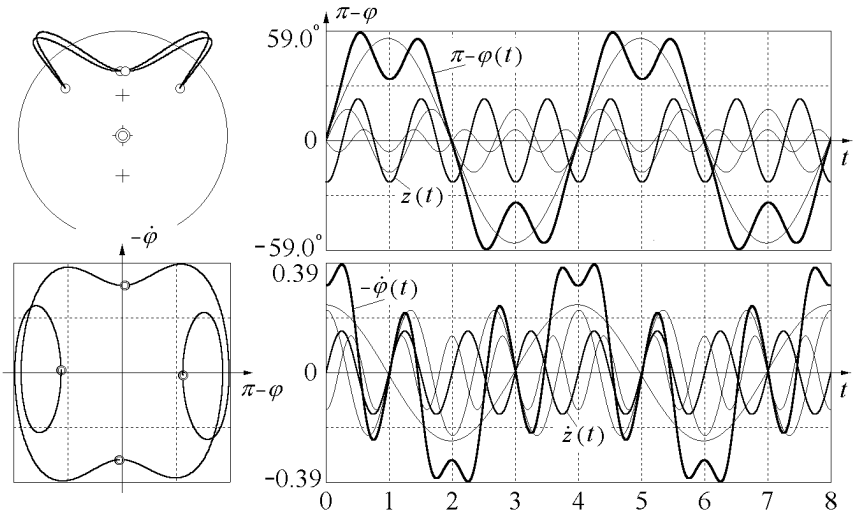

(quality 100, no gravity, axis amplitude 0.385, initial defl. 178.43 degr., init. ang. velocity -0.3104)

Figure 9. The spatial path, phase orbit, and graphs of period-4 oscillations. This example shows "double-nodding" oscillations about one of the dynamically stabilized equilibrium positions in the absence of gravity.

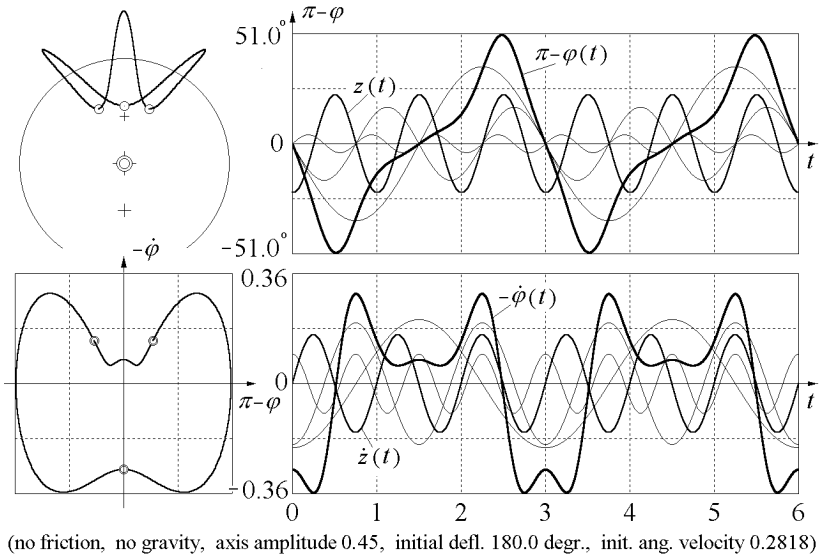

Figure 10. The spatial path, phase orbit, and graphs of period-3 oscillations.

amplitude steady-state oscillation (about the inverted vertical position) whose period is twice the driving period. This loss of stability of the inverted pendulum has been first described by Blackburn *et al.* [11] (the "flutter" mode) and demonstrated experimentally in [12]. The latest numerical investigation of the bifurcations associated with the stability of the inverted state can be found in [7]. The graphs and the double-lobed phase trajectory of such oscillations are shown in Figure 11.

Obviously, these steady-state oscillations can be regarded as a special case of subharmonic resonances, specifically, the case with $n = 2$. As we already mentioned, for small values of n it is impossible to correctly represent the pendulum motion as consisting of the slow and rapid components. The driving amplitude $a_{\max}$ is not small compared with the length l of the pendulum. Consequently, this case occurs beyond the limits of applicability of the approach based on the effective potential. This approach cannot explain the destabilization of the inverted pendulum, as well as the loss of stability of the hanging down pendulum at conditions of ordinary parametric resonance. (In the latter case the driving amplitude can be small, but the necessary driving frequency is not high enough for the separation of rapid and slow motions.)

However, the simulation shows (see Figure 11) a very simple spectral composition of period-2 steady oscillations occurring over the upper boundary of dynamic stability: the fundamental harmonic whose frequency equals $\omega/2$ (half the driving frequency ω) with a small addition of the third harmonic with the frequency $3\omega/2$. We note that large-amplitude oscillations of the non-inverted pendulum in conditions of the principal parametric resonance are characterized by a similar spectrum. This similarity of the spectra is by no means occasional: both the ordinary parametric resonance and the period-2 "flutter" mode that destroys the dynamic stability of the inverted state belong essentially to the same branch of possible steady-state period-2 oscillations of the parametrically excited pendulum. Therefore the upper boundary of dynamic stability for the inverted pendulum can be found directly from

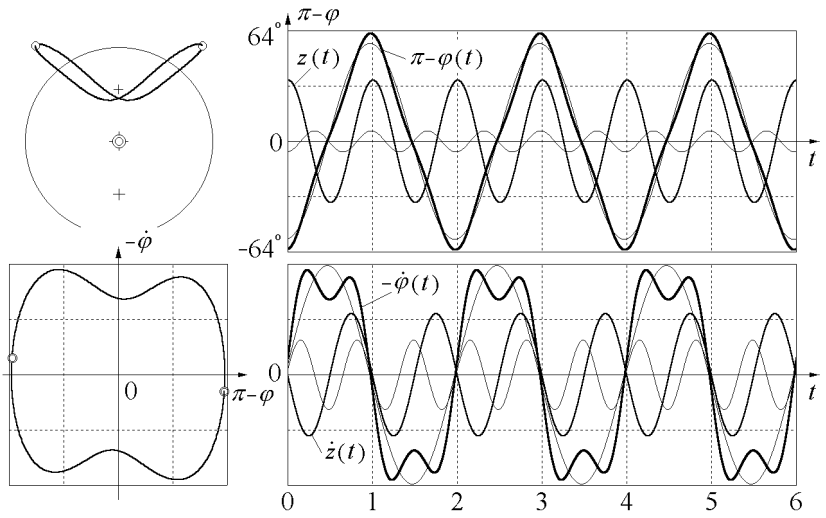

Figure 11. Stationary period-2 oscillations occurring over the upper boundary of dynamic stability (the "flutter" mode). The spectrum consists of the fundamental harmonic (frequency $\omega/2$) and the third harmonic (frequency $3\omega/2$).

the linearized differential equation of the system, equation (9), by the same method that is commonly used for determination of conditions which lead to the loss of stability of the non-inverted pendulum through excitation of ordinary parametric resonance (the ranges of parametric instability; see, for example, [10]). We can apply the linearized equation to this problem because at the boundary of dynamic stability the amplitude of oscillations is infinitely small. The periodic solution to equation (9), which corresponds to the boundary of instability, can be represented as a superposition of the fundamental harmonic whose frequency $\omega/2$ equals half the driving frequency, and the third harmonic with the frequency $3\omega/2$:

$$\varphi(t) = A_1 \sin(\omega t/2) + A_3 \sin(3\omega t/2). \tag{18}$$

Substituting $\varphi(t)$ from equation (18) into the linearized differential equation, equation (9), with $\gamma = 0$ and expanding the products of trigonometric functions, we obtain an expression, in which we should equate to zero the coefficients of $\sin(\omega t/2)$ and $\sin(3\omega t/2)$. Thus we get a system of homogeneous equations for the coefficients A_1 and A_3, which has a nontrivial solution when its determinant equals zero. This requirement yields a quadratic equation for the desired normalized critical driving amplitude $a_{\max}/l = m_{\max}$. The relevant root of this equation (in the case $\omega_0 = 0$ which corresponds to the absence of gravity or to the high frequency limit of the pivot oscillations with gravity) is $m_{\max} = 3(\sqrt{13} - 3)/4 = 0.454$, and the corresponding ratio of amplitudes of the third harmonic to the fundamental one equals $A_3/A_1 = (\sqrt{13}-3)/6 = 0.101$. A somewhat more complicated calculation in which the higher harmonics (up to the 7th) in $\varphi(t)$ are taken into account yields for $m_{\max}$ and A_3/A_1 the values that coincide (within the assumed accuracy) with those cited above. These values agree well with the simulation experiment in conditions of the absence of gravity ($\omega_0 = 0$) and very small angular excursion of the pendulum. When the

normalized amplitude of the pivot $m = a/l$ exceeds the critical value $m_{\max} = 0.454$, the swing of the period-2 "flutter" oscillation (amplitude A_1 of the fundamental harmonic) increases in proportion to the square root of this excess: $A_1 \propto \sqrt{a - a_{\max}}$. This dependence follows from the nonlinear differential equation of the pendulum, equation (5), if $\sin\varphi$ in it is approximated as $\varphi - \varphi^3/6$, and also agrees well with the simulation experiment for amplitudes up to 45°.

As the normalized amplitude $m = a/l$ of the pivot is increased over the value 0.555, the symmetry-breaking bifurcation occurs: The angular excursions of the pendulum to one side and to the other become different, destroying the spatial symmetry of the oscillation and hence the symmetry of the phase orbit. As the pivot amplitude is increased further, after $m = 0.565$ the system undergoes a sequence of period-doubling bifurcations, and finally, at $m = 0.56622$ (for $Q = \omega/2\gamma = 20$), the oscillatory motion of the pendulum becomes replaced, at the end of a very long chaotic transient, by a regular unidirectional period-1 rotation.

Similar (though more complicated) theoretical investigation of the boundary conditions for period-2 stationary oscillations in the presence of gravity allows us to obtain the dependence of the critical (destabilizing) amplitude m of the pivot on the driving frequency ω. In terms of $k = (\omega_0/\omega)^2$ this dependence has the following form:

$$m_{\max} = (\sqrt{117 - 232k + 80k^2} - 9 + 4k)/4. \tag{19}$$

The graph of this boundary is shown in Figure 3 by the curve marked as $n = 2$. The critical driving amplitude tends to zero as $k \to 1/4$ (as $\omega \to 2\omega_0$). This condition corresponds to ordinary parametric resonance of the hanging down pendulum: At small driving amplitudes this resonance is excited if the driving frequency equals the doubled natural frequency. If the driving frequency exceeds $2\omega_0$ (that is, if $k < 0.25$), a finite driving amplitude is required for infinitely small steady parametric oscillations even in the absence of friction.

The curve $n = 2$ intersects the ordinate axis at $m = 3(\sqrt{13} - 3)/4 = 0.454$. This case ($k = 0$) corresponds to the mentioned above limit of a very high driving frequency ($\omega/\omega_0 \to \infty$) or zero gravity ($\omega_0 = 0$), so that $m = 0.454$ gives the upper limit of stability for each of the two dynamically stabilized equivalent equilibrium positions. The continuation of this curve to the region of negative k values corresponds to the transition from ordinary downward gravity through zero to "negative," or upward "gravity," or, which is the same, to the case of inverted pendulum in ordinary (directed down) gravitational field. Thus, the same formula, equation (19), gives the driving amplitude (as a function of the driving frequency) at which both the equilibrium position of the hanging down pendulum is destabilized due to excitation of ordinary parametric oscillations, and the dynamically stabilized inverted equilibrium position is destabilized due to excitation of period-2 "flutter" oscillations. We can treat this as an indication that both phenomena are closely related and have common physical nature. All the curves that correspond to subharmonic resonances of higher orders ($n > 2$) lie between this curve and the lower boundary of dynamical stabilization of the inverted pendulum (curve $n \to \infty$ in Figure 3).

Actually, equation (19) in the vicinity of $k = 1/4$ ($\omega = 2\omega_0$) gives both boundaries of the instability interval that surrounds the principal parametric resonance. For $k > 1/4$ ($\omega < 2\omega_0$) equation (19) yields negative m whose absolute value $|m|$ corresponds to stationary oscillations at the other boundary (to the right of $k = 0.25$, see Figure 3). Such oscillations are also represented by two harmonic components with

frequencies $\omega/2$ and $3\omega/2$, but their phases differ from those in equation (18) – these harmonics are of cosine type (for $m > 0$). Periodic oscillations at this boundary are unstable and after some time either generate a chaotic process with random revolutions and oscillations (at sufficiently large driving amplitudes), or eventually come to a synchronized rotation or to steady (large amplitude) oscillations corresponding to the other (sine-type) stable branch. Such steady-state oscillations are almost purely sinusoidal even if they have a very large amplitude (exceeding 90 degrees).

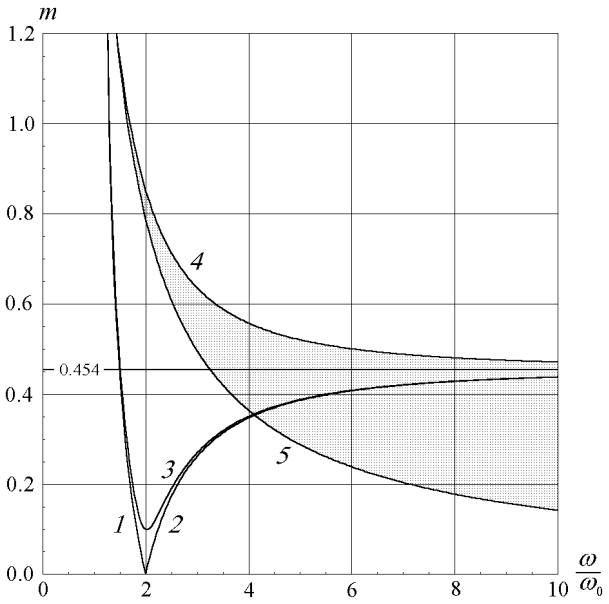

Figure 12. The boundaries of parametric instability – driving amplitude versus normalized driving frequency. *1* and *2* – boundaries of the principal interval of parametric instability ($\omega \approx 2\omega_0$) for the non-inverted pendulum in the absence of friction, *3* – the same with friction ($Q = 5.0$), *4* and *5* – the upper and lower boundaries of dynamic stability for the inverted pendulum.

The boundaries of the principal interval of parametric instability are shown by curves *1* and *2* in Figure 12 as functions of normalized driving frequency ω/ω_0 (instead of more convenient but physically less meaningful quantity $k = (\omega_0/\omega)^2$ used in Figure 3). For the hanging down pendulum, in the absence of friction the critical amplitude tends to zero as the frequency of the pivot approaches $2\omega_0$ from either side. Curve *3* shows in the parameters plane (ω/ω_0, a/l) the region of principal parametric resonance in the presence of friction (for $Q = \omega_0/2\gamma = 5.0$). The non-inverted vertical position of the pendulum whose pivot is vibrating at frequency $2\omega_0$ loses stability when the normalized amplitude of this vibration exceeds the threshold value of $1/2Q$. This curve almost merges with curves *1* and *2* as the frequency ω deviates from the resonant value $2\omega_0$. (Detailed discussion of the role of friction see below.) In the high-frequency limit, for which the role of gravity is negligible, the normalized critical pivot amplitude a/l tends to the value 0.454 that corresponds to destabilization of the two symmetric equilibrium positions in the absence of gravity.

Curve *4* of this diagram corresponds to destabilization of the inverted pendulum

by excitation of the "flutter" oscillations. The smaller the frequency of the pivot, the greater the critical amplitude at which the inverted position becomes unstable. Actually curve *4* for the boundary of the "flutter" mode is the continuation (through infinite values of the driving frequency) of curve *2* (or curve *3* in the presence of friction). The latter is the boundary of ordinary parametric resonance of the non-inverted pendulum. This relationship between the two phenomena becomes especially obvious if we compare curve *4* with its equivalent in Figure 3, which is the curve marked as $n = 2$ at negative k values.

Curve *5* in Figure 12 shows in the parameter plane the lower boundary of dynamic stabilization of the inverted pendulum, which is defined in this paper more precisely than earlier [see equation (12)]. The loss of stability at crossing this boundary occurs when the effective potential well corresponding to the inverted position has zero depth. Thus, the region of stability of the inverted pendulum occupies the shaded part of the parameter plane between curves *5* and *4*.

We note that complex n-periodic "multiple-nodding" oscillations (subharmonic resonances) with $n > 2$ occur at driving amplitudes below the critical value $m_{\max}$ and also occupy a region below curve *4* on the parameter plane. However, the existence of these asymptotic oscillatory states does not influence the local dynamic stability of the inverted equilibrium position as well as the stability of hanging down position because the pendulum can be trapped in the n-periodic motions only after a certain initial disturbance, when its initial state occurs within the corresponding domain of attraction – otherwise the pendulum comes to rest.

6. The influence of friction

For small (and moderate) driving amplitudes, the principal parametric resonance occurs at a driving frequency whose value is approximately twice the natural frequency: $\omega \approx 2\omega_0$. We can calculate the threshold of parametric excitation of the hanging down pendulum in condition of the principal resonance by equating the work done by the force of inertia during a cycle of a steady motion of the pendulum to the energy dissipated due to friction. (The work done by the potential gravitational force for a complete cycle of a periodic motion is zero.) For the calculation of the threshold, it is convenient to consider that the pivot's motion is described by $z(t) = -a \sin \omega t$ rather than by equation (1). This specific phase of the pivot's oscillation can be provided by an appropriate choice of the time origin. In this case the small steady oscillations at the threshold are approximately described by a cosine function: $\varphi(t) = c_1 \cos \omega t/2$.

The torque of the force of inertia is $F_{\text{in}} l \sin \varphi$, and the elementary work dW done by this torque during an infinitesimal time interval dt is $F_{\text{in}} l \sin \varphi d\varphi = F_{\text{in}} l \sin \varphi \, \dot{\varphi} dt = -I(a/l)\omega^2 \sin \omega t \sin \varphi \, \dot{\varphi} dt \approx -I(a/l)\omega^2 \sin \omega t \, \varphi \dot{\varphi} dt$, where I is the pendulum's moment of inertia. Integrating this expression over the period of the pendulum motion $T = 2\pi/\omega_0 = 4\pi/\omega$, we find the total work done during T, that is, the increment ΔE in the total energy E during two driving periods due to the parameter variation: $\Delta E = I\omega^2 c_1^2 (a/l)\omega/2\pi$.

The work of the frictional force determines the dissipation of mechanical energy. The elementary (negative) work dW done by the torque of this force during dt is $-2I\gamma(\dot{\varphi})^2 dt$. Integrating this work over the period of oscillation, we find $-I\gamma c_1^2 \omega^2 \pi$. Equating the absolute values of the works done by the force of inertia and the frictional force yields $\omega(a/l) = 2\gamma$. Since at resonance $\omega \approx 2\omega_0$, we obtain the following approximate expression for the threshold value of the normalized amplitude of the

pivot: $m_{\text{thres}} = a_{\text{thres}}/l = \gamma/\omega_0 = 1/2Q$.

If the threshold is exceeded, parametric resonance occurs not only when the driving frequency is exactly twice the natural frequency, but rather in some interval of driving frequencies extending on both sides of the resonant frequency $\omega_{\text{res}} = 2\omega_0$. For a given value of the driving amplitude, the interval the wider the smaller the friction. To find the boundaries of parametric instability in the presence of friction, we should include the damping term $2\gamma\dot{\varphi}$ in the linearized differential equation of the pendulum, equation (9). With friction, the solution to this equation includes, in contrast to equation (18), both sine and cosine terms:

$$\varphi(t) = A_1 \sin(\omega t/2) + A_3 \sin(3\omega t/2) + B_1 \cos(\omega t/2) + B_3 \cos(3\omega t/2). \tag{20}$$

Substituting $\varphi(t)$, equation (20), into equation (9), we obtain the homogeneous system of approximate equations for A_1, A_3, and B_1, B_3. Desired boundaries of parametric instability are found from the condition of existence of a non-trivial solution to this system. Expressions for the boundaries that follow from this calculation are rather complicated and not cited in this paper. The corresponding graph (for $Q = 5$) is shown by curve *3* in Figure 12. The structure of the boundaries in the vicinity of $\omega = 2\omega_0$ is shown in detail by three thick curves in Figure 13 for $Q = 5$, $Q = 10$, and for the absence of friction ($Q \to \infty$). If the driving parameters lie in the region inside these "tongues," the hanging equilibrium position is unstable, and the pendulum leaves it after a slightest perturbation. The growth of the amplitude is restricted by nonlinear effects (by dependence of the natural frequency on the amplitude).

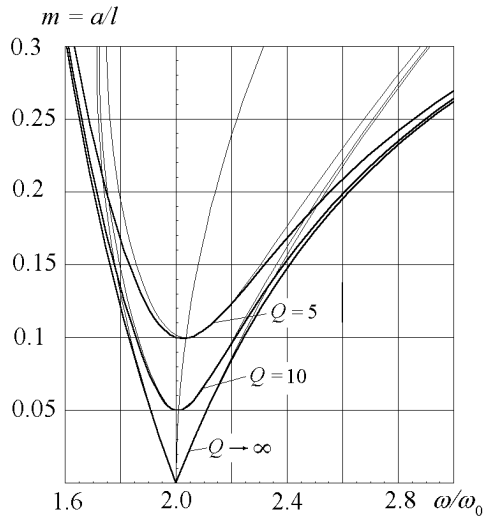

Figure 13. Boundaries of the principal interval of parametric instability for the hanging down pendulum with friction (normalized driving amplitude versus normalized driving frequency). Thin curves are plotted according to the approximate formula, equation (21).

Thin curves in Figure 13 are plotted according to the following approximate formula for the boundaries (valid for small driving amplitudes near $\omega = 2\omega_0$):

$$\omega_{1,2} = (2 \pm 2\sqrt{m^2 - 1/(2Q)^2} + 7m^2/2)\omega_0. \tag{21}$$

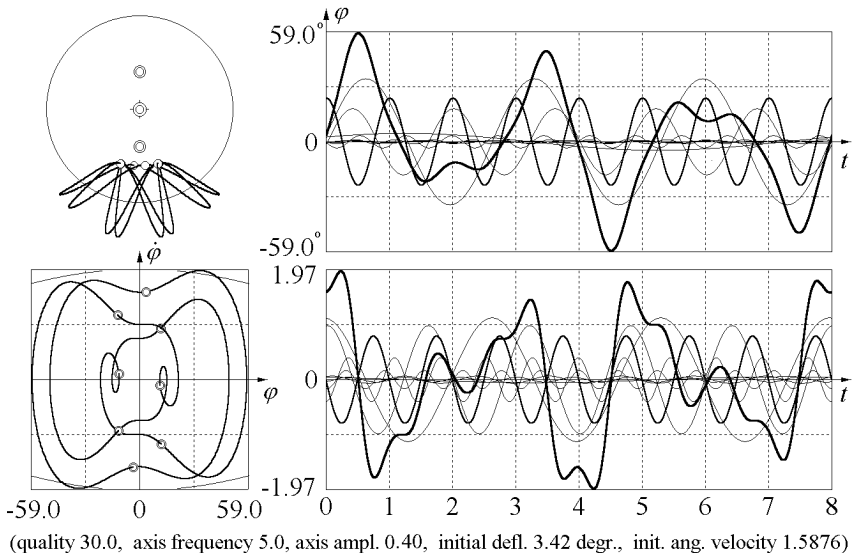

Figure 14. The spatial path, phase orbit, and graphs of stationary oscillations that can be treated as a subharmonic resonance of a fractional order 8/3. The third harmonic (frequency $3\omega/8$) dominates in the spectrum.

7. Subharmonic resonances of fractional orders

In this section we report about new modes of regular behaviour of the parametrically driven pendulum, kindred to the described above subharmonic resonances, which we have discovered recently in the simulation experiments. As far as we know, such modes haven't been described in the literature.

Figure 14 shows a regular period-8 motion of the pendulum, which can be characterized as a subharmonic resonance of a fractional order, specifically, of the order 8/3 in this example. Here the amplitude of the fundamental harmonic (whose frequency equals $\omega/8$) is much smaller than the amplitude of the third harmonic (frequency $3\omega/8$). This third harmonic dominates in the spectrum, and can be regarded as the principal one, while the fundamental harmonic can be regarded as its third subharmonic. Considerable contributions to the spectrum are given also by the 5th and 11th harmonics of the fundamental frequency. Approximate boundary conditions for small-amplitude stationary oscillations of this type ($n/3$-order subresonance) can be found analytically from the linearized differential equation by a method similar to that used above for n-order subresonance: we can try as $\varphi(t)$ a solution consisting of spectral components with frequencies $3\omega/n$, $(n-3)\omega/n$, and $(n+3)\omega/n$:

$$\varphi(t) = A_3 \sin(3\omega t/n) + A_{n-3} \sin[(n-3)\omega t/n] + A_{n+3} \sin[(n+3)\omega t/n]. \qquad (22)$$

Substituting this trial function $\varphi(t)$ into equation (9) (with $\gamma = 0$) and expanding the products of trigonometric functions, we obtain a system of equations for the coefficients A_3, A_{n-3} and A_{n+3}. Condition of existence of a non-trivial solution to

the system yields the following expression for the minimal driving amplitude:

$$m_{\min} = \frac{3\sqrt{2}(n^2 - 3^2)}{n^2\sqrt{n^2 + 3^2}}. \tag{23}$$

(Compare equation (23) with a similar expression, equation (13), for the critical driving amplitude of the integer-order subharmonic resonances.) The analytical results of calculations for $n \geq 8$ agree well with the simulations, especially if one more high harmonic is included in the trial function $\varphi(t)$. If the driving amplitude exceeds the critical value, the angular excursion of the pendulum at these modes increases, and additional harmonics appear in its spectrum.

8. Concluding remarks

The parametrically excited pendulum is richer in various modes of possible behaviour than we can expect for such a simple physical system relying on our intuition. Its nonlinear large-amplitude motions can hardly be called "simple." In this paper we have touched only a small part of existing motions. We have suggested a clear physical explanation of subharmonic resonances and developed an approximate quantitative theory of these modes. The spectral composition of subharmonic resonances is investigated quantitatively, and their low-amplitude boundaries in the parameter space are determined. Also several related modes of regular behaviour (subharmonic resonances of fractional orders) are described and explained for the first time.

The simulations show that variations of the parameter set (dimensionless driving amplitude a/l, normalized driving frequency ω/ω_0, and quality factor Q) result in numerous different regular and chaotic types of behaviour. The pendulum's dynamics exhibits a great variety of other asymptotic rotational, oscillatory, and combined (both rotational and oscillatory) multiple-periodic stationary states as well as chaotic attractors, whose basins of attraction are characterized by a surprisingly complex (fractal) structure. Computer simulations reveal also intricate sequences of bifurcations, leading to numerous complicated chaotic regimes. All these motions remained beyond the scope of this paper. With good reason we can suppose that this apparently simple physical system is inexhaustible.

References

[1] Butikov E I 1999 The rigid pendulum – an antique but evergreen physical model *Eur. J. Phys.* **20** 429 – 441
[2] McLaughlin J B 1981 Period-doubling bifurcations and chaotic motion for a parametrically forced pendulum *J. Stat. Physics* **24** (2) 375 – 388
[3] Koch B P, Leven R W, Pompe B, and Wilke C 1983 Experimental evidence for chaotic behavior of a parametrically forced pendulum *Phys. Lett.* A **96** (5) 219 – 224
[4] Leven R W, Pompe B, Wilke C, and Koch B P 1985 Experiments on periodic and chaotic motions of a parametrically forced pendulum *Physica* D **16** (3) 371 – 384
[5] Willem van de Water and Marc Hoppenbrouwers 1991 Unstable periodic orbits in the parametrically excited pendulum *Phys. Rev.* A **44** (10) 6388 - 6398
[6] Starrett J and Tagg R 1995 Control of a chaotic parametrically driven pendulum *Phys. Rev. Lett.* **74**, (11) 1974 – 1977
[7] Sang-Yoon Kim and Bambi Hu 1998 Bifurcations and transitions to chaos in an inverted pendulum *Phys. Rev.* E **58**, (3) 3028 – 3035
[8] Stephenson A 1908 On an induced stability *Phil. Mag.* **15** 233 – 236, On a new type of dynamical stability *Mem. Proc. Manch. Lit. Phil. Soc.* **52** (8) 1 – 10

[9] Kapitza P L 1951 Dynamic stability of the pendulum with vibrating suspension point *Soviet Physics – JETP* **21** , (5) 588 – 597 (in Russian), see also *Collected papers of P. L. Kapitza* edited by D. Ter Haar, Pergamon, London (1965), v. 2, pp. 714 – 726.
[10] Landau L D and Lifschitz E M 1988 *Mechanics* Nauka Publishers, Moscow (in Russian), *Mechanics* Pergamon, New York (1976) pp. 93 - 95.
[11] Blackburn J A, Smith H J T, Groenbech-Jensen N 1992 Stability and Hopf bifurcations in an inverted pendulum *Am. J. Phys.* **60** (10) 903 – 908
[12] Smith H J T, Blackburn J A 1992 Experimental study of an inverted pendulum *Am. J. Phys.* **60** (10) 909 – 911
[13] Acheson D J 1995 Multiple-nodding oscillations of a driven inverted pendulum *Proc. Roy. Soc. London* **A 448** 89 – 95
[14] Grandy W T Jr, Schöck M 1997 Simulations of nolinear pivot-driven pendula *Am. J. Phys.* **65** (5) 376 – 381
[15] Fenn Julia G, Bayne D A, and Sinclair B D 1998 Experimental investigation of the 'effective potential' of an inverted pendulum *Am. J. Phys.* **66** (11) 981 – 984
[16] Clifford M J and Bishop S R 1998 Inverted oscillations of a driven pendulum *Proc. Roy. Soc. London* A **454** 2811 – 2817
[17] Sudor D J, Bishop S R 1999 Inverted dynamics of a tilted parametric pendulum *Eur. J. Mech. A/Solids* **18** 517 – 526
[18] Bishop S R, Sudor D J 1999 The 'not quite' inverted pendulum *Int. Journ. Bifurcation and Chaos* **9** (1) 273 – 285
[19] Butikov E I 2002 *The parametrically driven pendulum* (the simulation program) http://www.ifmo.ru/butikov/Inverted.html
[20] Butikov E I 2001 On the dynamic stabilization of an inverted pendulum *Am. J. Phys.* **69** (7) 755 – 768